N87-27624

Computational Mechanics Institute
9th INTERNATIONAL CONFERENCE
BOUNDARY ELEMENT METHODS IN ENGINEERING
Stuttgart, 31 Aug-4 Sept 1987

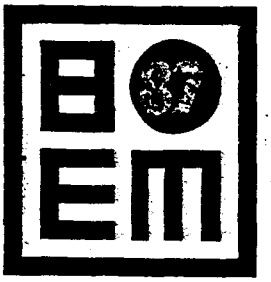

P-15

TRANSONIC AIRFOIL COMPUTATION USING THE INTEGRAL EQUATION WITH AND WITHOUT EMBEDDED EULER DOMAINS

OSAMA A. KANDIL AND HONG HU

DEPARTMENT OF MECHANICAL ENGINEERING AND MECHANICS
OLD DOMINION UNIVERSITY, NORFOLK, VA 23508, USA

TRANSONIC AIRFOIL COMPUTATION USING THE INTEGRAL EQUATION WITH AND WITHOUT EMBEDDED EULER DOMAINS

Osama A. Kandil and Hong Hu

Department of Mechanical Engineering and Mechanics,
Old Dominion University, Norfolk, VA 23508, USA

INTRODUCTION

Computation of the transonic flow around airfoils and wings using finite-difference and finite-volume methods requires fine grids and large computational domains around the source of disturbance. The outer boundary of the computational domain is usually placed at several chord lengths away from the inner boundary. Moreover, special treatment is required at the outer boundary to approximately satisfy the farfield boundary conditions. Using different levels of approximations, inviscid computational schemes have been developed based on the Transonic Small Perturbation (TSP) equation (Murman and Cole[1]; Edwards, Bland and Siedel[2]), Full Potential (FP) equation (Steger and Lomax[3]; Garabedian and Korn[4]; Jameson[5]) and Euler equation (Jameson[6]). These schemes require large capacity of computer memory to handle the large number of grid points and the associated flow variables. They also require large CPU time to obtain converged solutions due to the large number of iteration cycles —— usually it is of order a thousand.

The potential equations can be used for flows with weak schocks since the entropy increase and vorticity production across these shocks are small. For strong shocks, the irrotational and isentropic flow assumptions are invalid and one cannot use the potential flow equations across or behind the shocks. For these flows, one has to correct the potential equations in order to include the entropy jump across the shock wave. Methods of this type have been developed by Hafez and Lovell[7], Fuglsang and Williams[8] and Whitlow, Hafez and Osher[9]. Alternatively, one has to use the computationally

more expensive Euler equations.

The Integral Equation Formulation (IEF) using the TSP (Piers and Sloof[10]; Tseng and Morino[11]) or the FP (Kandil and Yates[12]; Oskam[13]; Erickson and Strande[14]; Sinclair[15]; Kandil and Hu[16]) equations represents an alternative to the finite difference and finite volume methods to treat transonic flows with weak shocks. With the IEF, the farfield boundary conditions are automatically satisfied and only a small computational domain is needed around the source of disturbance. Moreover, the accuracy of the method depends on the evaluation of integrals rather than derivatives and hence coarse grids can be used within the small computational domain. Because of these obvious advantages of the methods which are based on the IEF, it is highly desirable to fully develop these methods and extend them to treat transonic flows over a wide range of Mach numbers.

In this paper, we present a transonic integral equation method which is based on the full potential equation, and couple the method with embedded Euler domains to treat strong shocks. The method is extensively applied to different airfoil sections and Mach numbers. The results are compared with experimental data and other results which were obtained by using finite-difference and finite-volume methods with TSP, FP and Euler equations.

FORMULATION

Full Potential Equation

For transonic flows with weak shocks, the dimensionless governing equations of the two-dimensional, steady, potential flow are given by

$$\Phi_{xx} + \Phi_{yy} = G \tag{1}$$

$$G = \frac{-1}{\rho} (\rho_x \Phi_x + \rho_y \Phi_y) \tag{2}$$

$$\rho = [1 + \frac{\gamma-1}{2} M_\infty^2 (1 - \Phi_x^2 - \Phi_y^2)]^{1/\gamma-1} \tag{3}$$

where Φ is the total velocity potential, ρ the density, M_∞ the freestream Mach number, γ the ratio of specific heats and the subscripts x and y refer to the derivatives. It should be noted that G represents the total compressibility in the flow. The characteristic parameters are the freestream velocity (U_∞) and density (ρ_∞) and the airfoil chord length (ℓ).

The boundary conditions on the airfoil g, away from g and at the trailing edge TE are given by

$$\nabla\Phi \cdot \hat{n} = 0 \qquad \text{on } g(x, y) = 0 \tag{4}$$

$$\nabla\Phi \to \bar{e}_\infty \qquad \text{away from g} \tag{5}$$

$$\Delta C_p\Big|_{TE} = 0 \tag{6}$$

where $\hat{n} = \nabla g/|\nabla g|$, $\bar{e}_\infty$ is a unit vector parallel to $\bar{U}_\infty$ and ΔC_p is the pressure jump. The pressure coefficent is given by

$$C_p = \frac{2}{\gamma M_\infty^2}\left\{\left[1 + \frac{\gamma-1}{2} M_\infty^2 (1 - \Phi_x^2 - \Phi_y^2)\right]^{\gamma/\gamma-1} - 1\right\} \tag{7}$$

The formal solution of Eq. (1) in terms of the velocity field $\nabla\Phi$ with explicit contribution of the shock surface S is obtained as

$$\nabla\Phi(x,y) = \bar{e}_\infty + \frac{1}{2\pi}\oint_g q_g(s)\,\frac{(x-\xi)\,\bar{i} + (y-\eta)\,\bar{j}}{(x-\xi)^2 + (y-\eta)^2}\,ds$$

$$+ \frac{1}{2\pi}\oint_g \gamma_g(s)\,\frac{(y-\eta)\,\bar{i} - (x-\xi)\,\bar{j}}{(x-\xi)^2 + (y-\eta)^2}\,ds$$

$$+ \frac{1}{2\pi}\iint G(\xi,\eta)\,\frac{(x-\xi)\,\bar{i} + (y-\eta)\,\bar{j}}{(x-\xi)^2 + (y-\eta)^2}\,d\xi d\eta$$

$$+ \frac{1}{2\pi}\oint_S q_S(s)\,\frac{(x-\xi)\,\bar{i} + (y-\eta)\,\bar{j}}{(x-\xi)^2 + (y-\eta)^2}\,ds \tag{8}$$

where q_g and γ_g are the airfoil surface distributions of sources and vorticity; respectively, and q_S is the source strength of the shock surface. In the shock-capturing scheme, the last integral term in Eq. (8) is dropped, since this term is included in the third integral term of the equation. In the shock capturing-shock fitting scheme, the last integral term corresponding to the shock surface is retained when shock fitting is used. For shock fitting, the following equations are used to determine the shock strength q_S, properties behind

the shock ρ_2, V_{2n}, V_{2t} and the orientation of the segments forming the shock surface β:

$$q_S = -(V_{1n} - V_{2n}) = -\frac{2\,V_{1n}}{\gamma+1}\left(1 - \frac{1}{M_{1n}^2}\right) \quad , M_{1n} > 1 \tag{9}$$

$$V_{2n} = \frac{(\gamma-1)\,M_{1n}^2 + 2}{(\gamma+1)\,M_{1n}^2}\,V_{1n} \tag{10}$$

$$V_{2t} = V_{1t} \tag{11}$$

$$\rho_2 = \frac{(\gamma+1)\,M_{1n}^2}{(\gamma-1)\,M_{1n}^2 + 2}\,\rho_1 \tag{12}$$

$$\beta = \sin^{-1}\left[\frac{1.2\,\sin\beta\,\sin\theta}{\cos\,(\beta-\theta)} + \frac{1}{M_1^2}\right]^{1/2} \tag{13}$$

$$M_1 = M_\infty\,\left|\nabla\Phi\right|_1/\rho_1^{\frac{\gamma-1}{2}} \quad , \quad M_{1n} = M_\infty\,\nabla\Phi_1 \cdot \hat{n}_S/\rho_1^{\frac{\gamma-1}{2}} \tag{14}$$

where the subscripts 1 and 2 refer to the conditions ahead and behind the shock, respectively, while n and t refer to the normal and tangential directions to the shock surface S, respectively, and θ is the relative direction of the flow behind the shock to that ahead of the shock.

Euler Equations

For strong shocks, an embedded computational domain is constructed around the shock which has been preliminary found by the Integral solution with shock capturing only. With the boundary and initial conditions found from the Integral solution, the unsteady conservative form of the Euler equations are solved in this limited domain with psuedo time marching. The dimensionless conservative form of these equations is given by

$$\frac{\partial \bar{q}}{\partial t} + \frac{\partial \bar{E}}{\partial x} + \frac{\partial \bar{F}}{\partial y} = 0 \tag{15}$$

where the flow vector field $\bar{q}$ and the flux components $\bar{E}$ and

$\bar{F}$ are given by

$$\bar{q} = [\rho, \rho u, \rho v, \rho e]^t \tag{16}$$

$$\bar{E} = [\rho u, \rho u^2 + p, \rho uv, \rho uh]^t \tag{17}$$

$$\bar{F} = [\rho v, \rho uv, \rho v^2 + p, \rho vh]^t \tag{18}$$

The total energy and enthalpy per unit mass are given by

$$e = \frac{p}{(\gamma+1)\rho} + (u^2 + v^2)/2, \quad h = e + p/\rho \tag{19}$$

Since we are interested in the steady flow solution only, the energy equation [last elements in Eqs. (16)-(18)], which is a differential equation, is replaced by the algebraic steady form which states that the total enthalpy is constant. Hence, the energy equation is replaced by

$$p = (\rho/\gamma)\ [1/M_\infty^2 + (\gamma-1)\ (1 - u^2 - v^2)/2] \tag{20}$$

METHOD OF SOLUTION

Shock-Capturing Shock-Fitting (SCSF) Scheme

The basic difference between the incompressible Integral Equation Solution and the transonic Integral Equation Solution are the additional third and fourth integral terms of Eq. (8). In the shock capturing part of the scheme, the fourth integral term is dropped while in the shock fitting part of the scheme this term is taken into account.

The SCSF-scheme is an iterative scheme due to the nonlinearity of the third and fourth integral terms. The iterative scheme is described below:

Neglecting the fourth integral term and setting $G = 0$, a standard panel computation is used to obtain q_g and/or γ_g. The q_g and γ_g are piecewise linear distributions on each surface panel and they are defined in terms of their nodal values. Initial values of G are calculated at the centroids of the field elements by using the linear compressibility relation $G = M_\infty^2\, u_x$, where u_x is the x-derivative of the x-component of the velocity. The centroidal value G represents

the G value for the field element. Equation (8) is then used to enforce the surface boundary conditions, Eqs. (5) and (7) to find new q_g and/or γ_g. The density ρ and nonlinear compressibility G are calculated by using Eqs. (3) and (2). A type finite-difference expression is used to calculate ρ_x and ρ_y depending on the type of the centroidal point-subsonic or supersonic. Once the G values are obtained, the surface boundary conditions are satisfied again. The iterative procedure is continued until the shock location is fixed. This is the shock capturing part of the scheme.

Shock panels are then introduced at the shock location, the fourth itegral term of Eq. (8) is now taken into account, Eqs. (9) and (13) are used to calculate q_s and β and Eqs. (10)-(12) are used to cross the shcok panel. The iterative procedure is continued as before with the exception of dealing with the shock panels as explained. Convergence is achieved once the surface pressure converges. This is the shock fitting part of the scheme.

Integral Equation With Embedded Euler (IEEE) Scheme

In this scheme, the shock capturing part of the SCSF-scheme is used to locate the shock. Once the shock is captured, a fine grid is constructed within a small computational region around the shock where a finite-volume Euler scheme is used. The basic finite-volume equation is obtained by integrating Eq. (15) over x and y to obtain

$$\iint \frac{\partial q}{\partial t}\, dA + \oint (E\, dy + F\, dx) = 0 \qquad (21)$$

Equation (21) is then applied to each cell of the embedded grid of the Euler domain. The resulting difference equation is

$$\left(\frac{\partial q}{\partial t}\right)_{ij} \Delta A_{ij} + \sum_{r=1}^{4} (E\, \Delta y_r + F\, \Delta x_r) = 0 \qquad (22)$$

where ΔA is the cell area, r refers to the cell-side number and the integer subscripts i, j refer to the centroidal values. The Euler solver is a central-difference finite-volume method which uses four-stage Runge-Kutta time stepping with explicit second- and fourth-order dissipation terms. The details of this solver are given in reference [17].

The boundary and initial conditions for the Euler domain are obtained from the Integral equation solution which is interpolated on the Euler domain grid. The Euler solver is

then used to capture the shock and calculate the flow vector field $\underline{q}$. It should be emphasized here that the downstream boundary condition must be updated while Euler calculations are excuted. Fixing the $\underline{q}$ values of the Euler domain, the IE calculation is used to update the boundary conditions for the Euler domain. The iterative procedure is repeated until convergence is achieved.

COMPUTATIONAL EXAMPLES

In this section, we present applications of the SCSF- and IEEE-schemes to the NACA 0012 and 64A010A. According to the convergence study using different sizes of the IE computational domain, which was presented by the authors (Kandil and Hu[16]), a computational domain of 2 x 1.5, in the x and y directions, has been used around the airfoil in all the following applications. A rectangular grid of 64 x 60 has been used for the IE computation. The grid is clustered in the leading edge, the shock region and near the airfoil surface. Since the third integral term of Eq. (8) is computationally expensive, its computation with constant G distribution has been restricted to the nearfield computation. For the farfield computation, this term is replaced by the equivalent lumped source term at its centroid. With sufficient accuracy, it has been computationally determined that the nearfield distance from the centroid is ≤ 0.5.

Figure 1 shows the results of the SCSF-scheme for NACA 0012, $M_\infty = 0.8$ and $\alpha = 0^0$, along with comparisons with the computational results of Garabedian, Korn and Jameson[18], and the experimental data taken from reference 19. The SCSF scheme took 12 iteration cycles of shock capturing (SC) and 13 cycles of shock fitting (SF) to achieve convergence.

Figure 2 shows the results of the IEEE-scheme for the same case along with a comparison with the computational results of Jameson[6] who also used the finite-volume Euler scheme with four-stage Runge Kutta time stepping. In the present IEEE-scheme, the embedded Euler domain has a size of 0.5 x 0.6 around the shock region with a grid of 25 x 30. This case took 10 iteration cycles of SC, 250 time cycles of Euler iterations to achieve a residual error of 10^{-3} and 5 IE cycles to update the Euler domain boundary conditions.

Figures 3 and 4 show the results of the SCSF- and IEEE-schemes for NACA 64A010A, $M_\infty = 0.796$, $\alpha = 0^0$ along with comparisons with the computational results of Edwards, Bland and Seidel[2] who used the TSP equation, and the experimental data taken from reference 2. With the SCSF-scheme, the

numbers of SC and SF iteration cycles to achieve convergence are the same as those of the case presented in Fig. 1. With the IEEE-scheme, the embedded Euler domain has a size of 0.7 x 0.6 with a grid size of 35 x 30. This case, Fig. 4, took 10 iteration cycles of SC, 130 time cycles of Euler iterations to achieve a residual error of 10^{-3} and 3 IE cycles to update the Euler domain boundary conditions.

Figures 5 and 6 show the results of the SCSF- and IEEE-schemes for the lifting case of NACA 0012, $M_\infty = 0.75$ and $\alpha = 2^0$ along with the computational results of Steger and Lomax[3], and the experimental data taken from the same reference. The size of the grids and the number of iteration cycles used to achieve convergence are the same as those of the cases given in Fig. 1 and 2.

Figure 7 shows the results of the IEEE for NACA 0012, $M_\infty = 0.812$ and $\alpha = 0^0$ along with the experimental data of reference 18. In Fig. 8, the results of the IEEE for NACA 0012, $M_\infty = 0.82$ and $\alpha = 0^0$ are shown along with the three-dimensional solution at the wing root chord of Tseng and Morino[11], who use the IE for the TSP, and the experimental results of reference 20. The size of the embedded Euler domain for these cases is 0.8 x 0.8 and the computational grid is 40 x 40.

CONCLUDING REMARKS

Two transonic computational schemes which are based on the Integral Equation Formulation of the full potential equation have been presented. The first scheme is a Shock Capturing-Shock Fitting (SCSF) scheme which uses the full potential equation throughout with the exception of the shock wave where the Rankine-Hugoniot relations are used to cross and fit the shock. The second scheme is an Integral Equation with Embedded Euler (IEEE) scheme which uses the full potential equation with an embedded region where Euler equations are used. The two schemes are applied to several transonic airfoil flows and the results have been compared with numerous computational results and experimental data. The two schemes are nevertheless efficient as compared to the other existing schemes which use finite-difference or finite-volume methods throughout large computational domains with fine grids. The SCSF-scheme is restricted to flows with weak shocks, while the IEEE-scheme can handle strong shocks. Currently, the IEEE scheme is applied to other transonic flows with strong shocks as well as to unsteady pitching oscillations.

ACKNOWLEDGEMENT

This research work is supported by NASA Langley Research Center under Grant No. NAG-1-648.

REFERENCES

1. Murman, E. M. and Cole, J. D. (1971), Calculation of Plane Steady Transonic Flows, AIAA Journal, Vol. 9, pp. 114-121.

2. Edwards, J. W., Bland, S. R. and Seidel, D. A. (1984), Experience with Transonic Unsteady Aerodynamic Calculations, NASA TM 86278, Langley Research Center, Hampton, VA.

3. Steger, J. L. and Lomax, H. (1972), Transonic Flow about Two-Dimensional Airfoils by Relaxation Procedures, AIAA Journal, Vol. 10, pp. 49-54.

4. Garabedian, P. R. and Korn, D. (1972), Analysis of Transonic Airfoils, Comm. Pure Appl. Math, Vol. 24, pp. 841-851.

5. Jameson, A. (1974), Iterative Solution of Transonic Flows Over Airfoils and Wings, Comm. Pure Appl. Math., Vol. 27, pp. 283-309.

6. Jameson, A. (1982), Transonic Airfoil Calculations Using the Euler Equations. Numerical Methods in Aeronautical Fluid Dynamics (Ed. P. L. Roe), pp. 289-309, Academic Press, London and New York.

7. Hafez, M. and Lovell, D. (1983), Entropy and Vorticity Corrections for Transonic Flows, AIAA Paper 83-1926.

8. Fuglsang, D. F. and Williams, M. H. (1985), Non-Isentropic Unsteady Transonic Small Disturbance Theory, AIAA Paper 85-0600.

9. Whitlow, W., Jr., Hafez, M. M. and Osher, S. J. (1986), An Entropy Correction Method for Unsteady Full Potential Flows with Strong Shocks, NASA TM 87769, Langley Research Center, Hampton, VA.

10. Piers, W. J. and Sloof, J. W. (1979), Calculations of Transonic Flow by Means of a Shock-Capturing Field Panel Method, AIAA Paper 79-1459.

11. Tseng, K. and Morino, L. (1982), Nonlinear Green's Function Methods for Unsteady Transonic Flows. Transonic Aerodynamics (edited by D. Nixon), pp. 565-603, AIAA, New York.

12. Kandil, O. A. and Yates, E. C., Jr. (1986), Computation of Transonic Vortex Flows Past Delta Wings - Integral Equation Approach, AIAA Journal, Vol. 24, pp. 1729-1736.

13. Oskam, B. (1985), Transonic Panel Method for the Full Potential Equation Applied to Multicomponent Airfoils, AIAA Journal, Vol. 23, pp. 1327-1334.

14. Erickson, L. L. and Strande, S. M. (1985), A Theoretical Basis for Extending Surface - Paneling Methods to Transonic Flow, AIAA Journal, Vol. 23, pp. 1860-1867.

15. Sinclair, P. M. (1986), An Exact Integral (Field Panel) Method for the Calculation of Two-Dimensional Transonic Potential Flow Around Complex Configurations, Aeronautical Journal, June/July, pp. 227-236.

16. Kandil, O. A. and Hu, H. (1987), Integral Equation Solution for Transonic and Subsonic Aerodynamics, Third GAMM Seminar on Panel Methods in Mechanics, Kiel, FRG.

17. Kandil, O. A. and Chuang, A. (1986), Influence of Numerical Dissipation in Computing Supersonic Vortex-Dominated Flows, AIAA Paper 86-1073. Also to appear in AIAA Journal, Vol. 25.

18. Garabedian, P., Korn, D. G. and Jameson (1972), Supercritical Wing Sections, Lecture Notes in Economic and Mathematical Systems, Vol. 66.

19. Hall, M. G. (1975), Transonic Flows, IMA, Controller, HMSO, London.

20. Lee, K. D., Dickson, L. J., Chen, A. W. and Rubbert, P. E. (1978), An Improved Matching Method for Transonic Computations, AIAA Paper 78-1116.

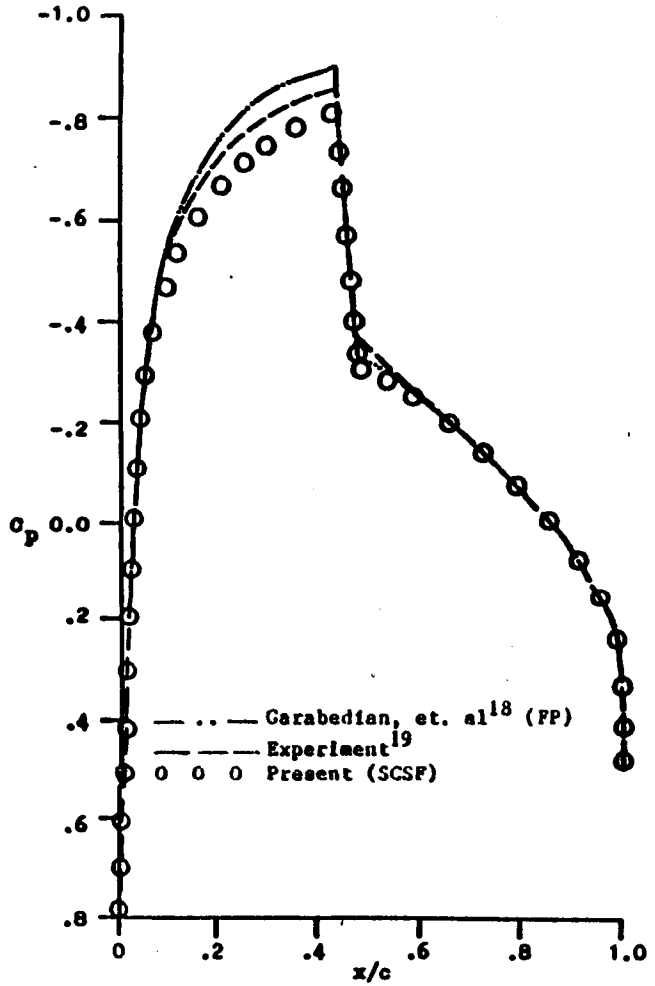

Fig. 1 Integral Eq. Solution with SCSF-Scheme, NACA 0012, $M_\infty = 0.8$, $\alpha = 0^0$.

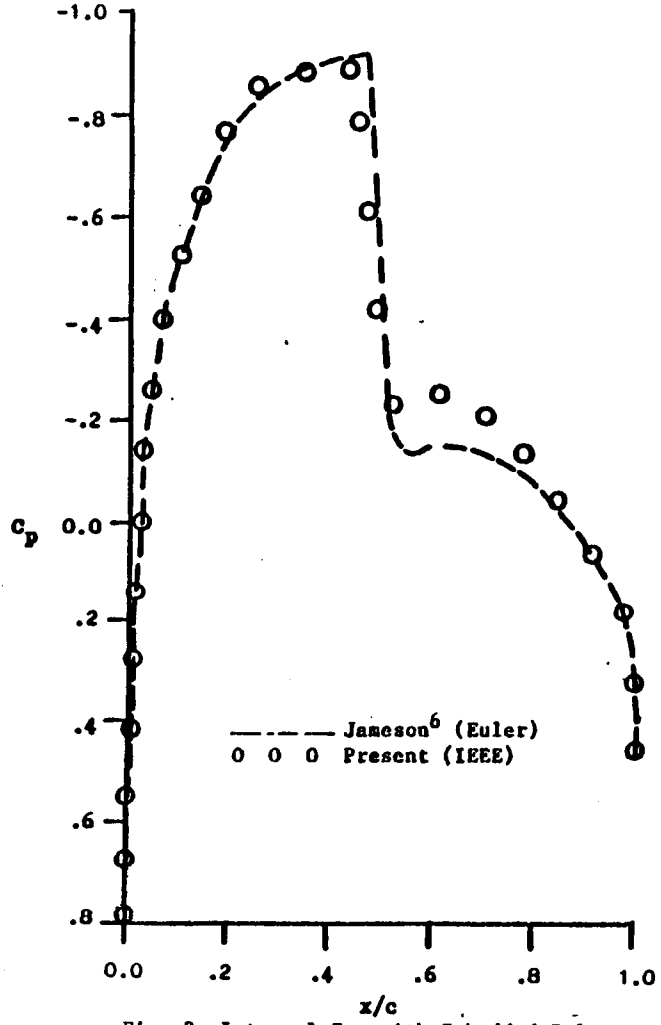

Fig. 2 Integral Eq. with Embedded-Euler Domain Solution, NACA 0012, $M_\infty = 0.8$, $\alpha = 0^0$.

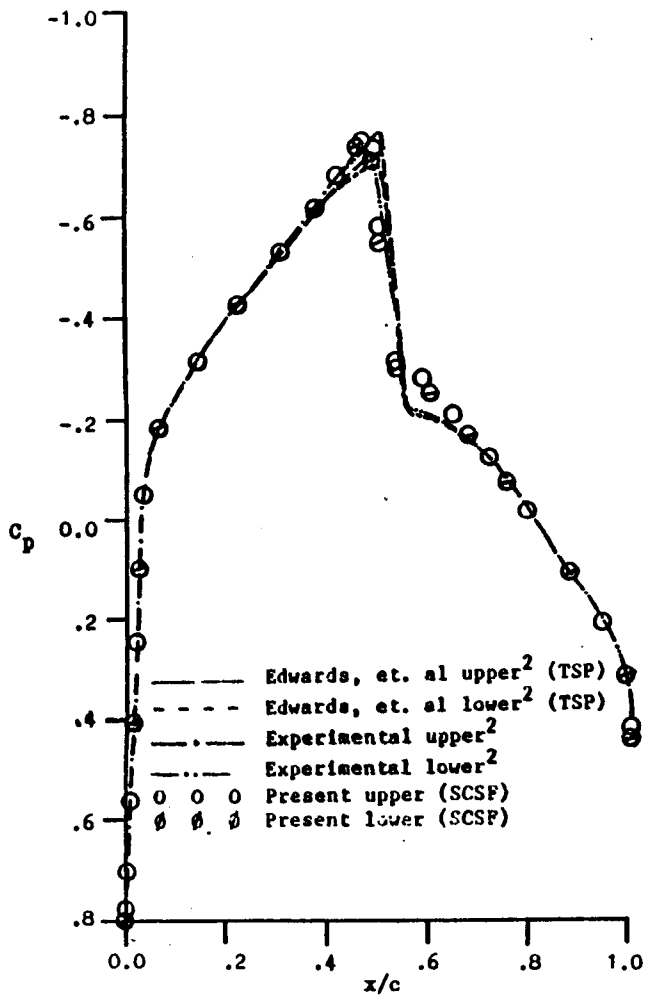

Fig. 3 Integral Eq. Solution with SCSF-Scheme, NACA 64A010A, $M_\infty = 0.796$, $\alpha = 0^0$.

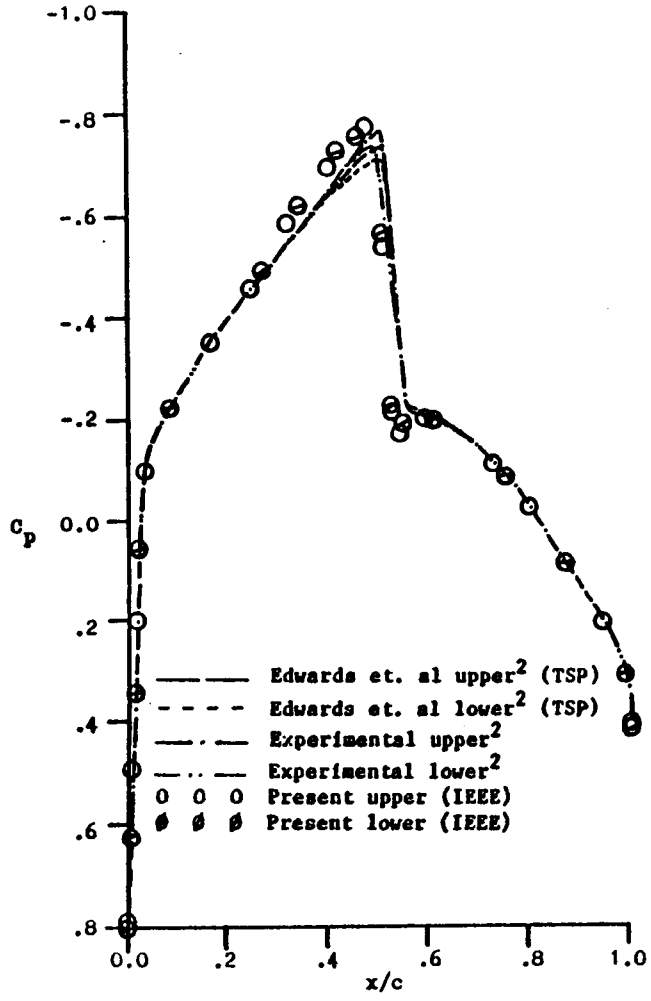

Fig. 4 Integral Eq. with Embedded-Euler Domain Solution, NACA 64A010A, $M_\infty = 0.796$, $\alpha = 0^0$.

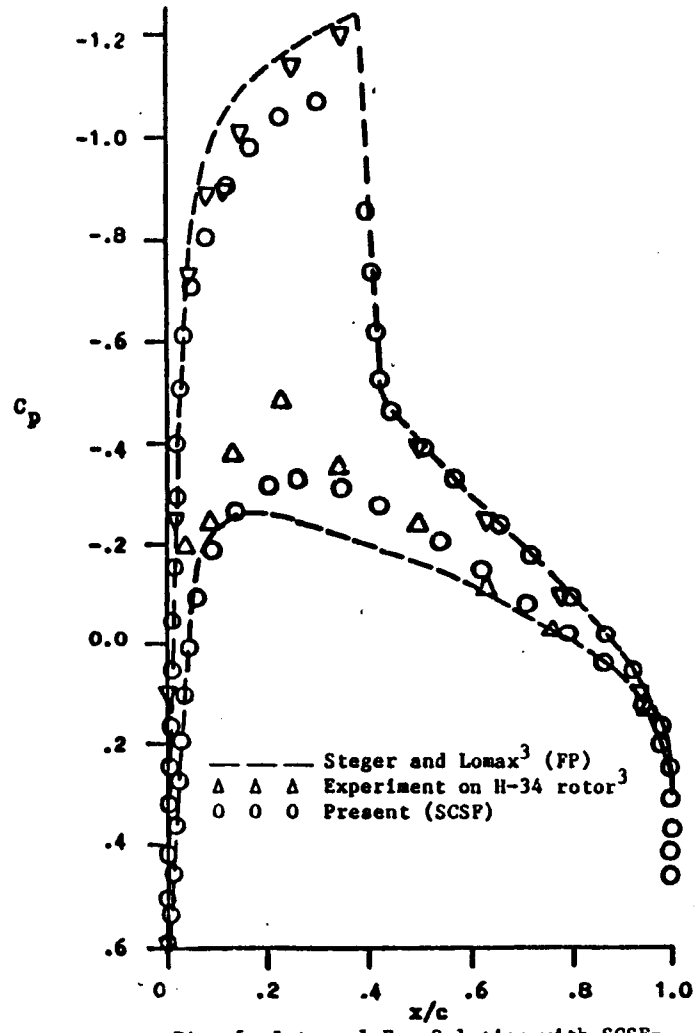

Fig. 5 Integral Eq. Solution with SCSF-Scheme, NACA 0012, $M_\infty = 0.75$, $\alpha = 2^0$.

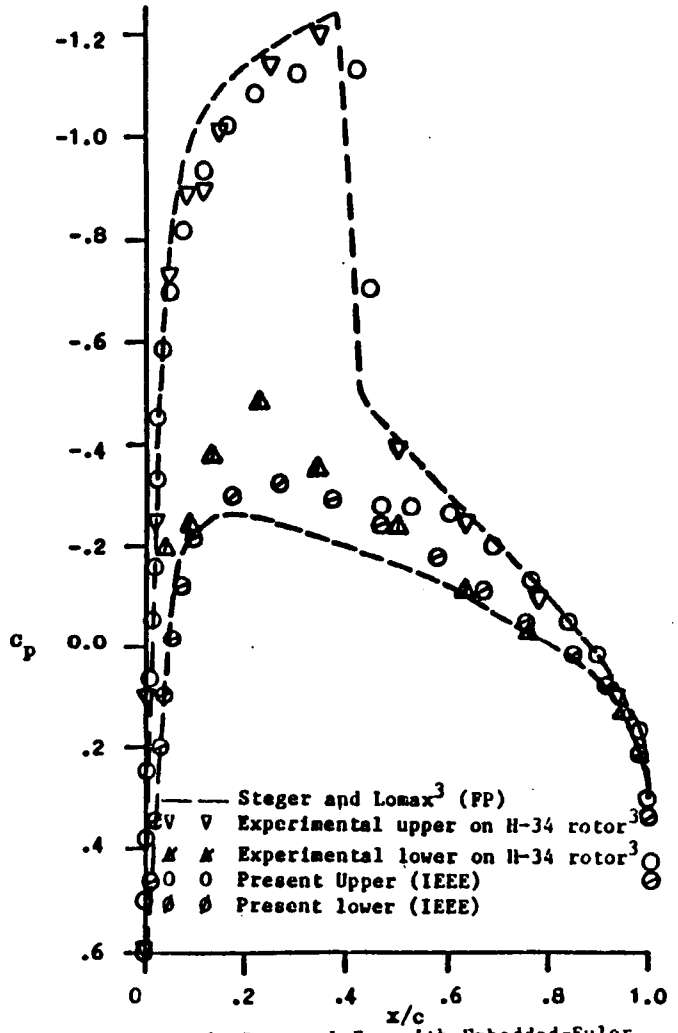

Fig. 6 Integral Eq. with Embedded-Euler Domain Solution, NACA 0012, $M_\infty = 0.75$, $\alpha = 2^0$.

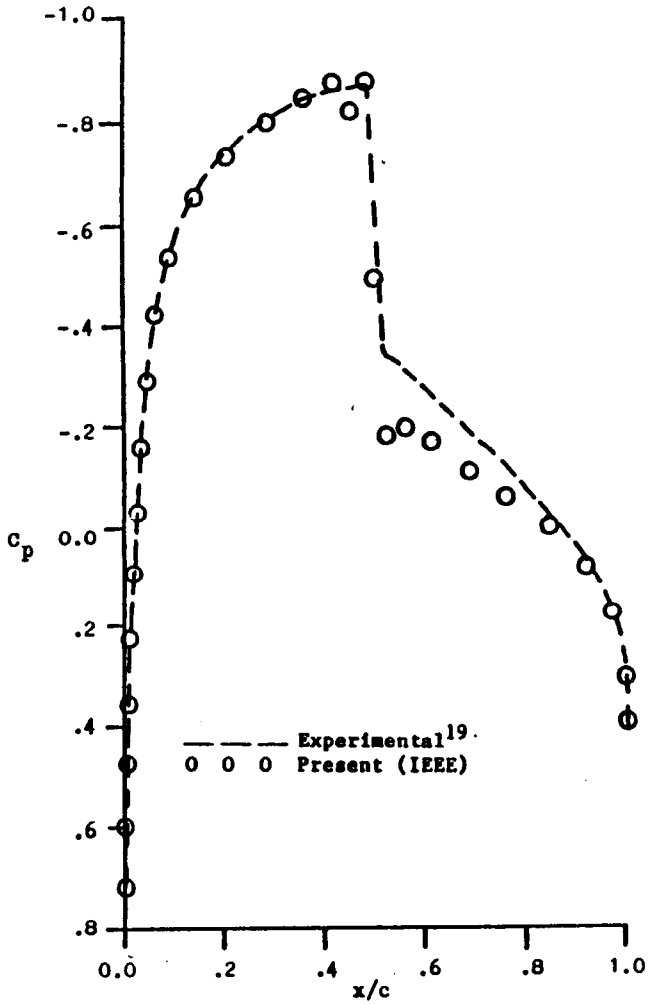

Fig. 7 Integral Eq. with Embedded-Euler Domain Solution, NACA 0012, $M_\infty = 0.812$, $\alpha = 0^0$.

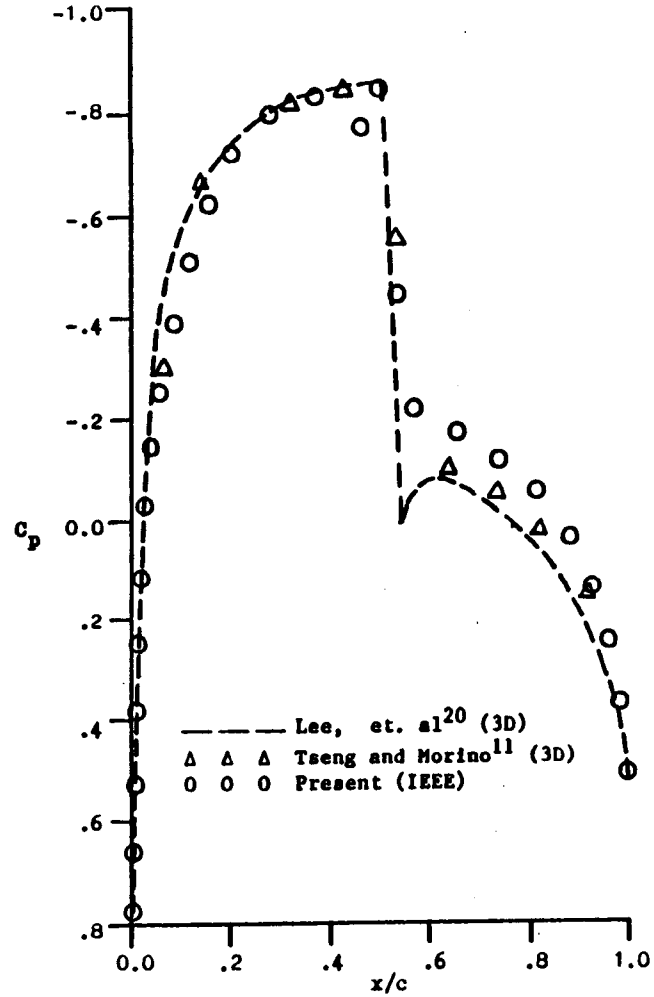

Fig. 8 Integral Eq. with Embedded-Euler Domain Solution, NACA 0012, $M_\infty = 0.82$, $\alpha = 0^0$.